

Rapid Degradation of Azo Dye by Fe-Based Metallic Glass Powder

Jun-Qiang Wang,* Yan-Hui Liu,* Ming-Wei Chen, Guo-Qiang Xie,
Dmitri V. Louzguine-Luzgin, Akihisa Inoue, and John H. Perepezko

The outstanding efficiency of Fe-based metallic glass powders in degrading organic water contaminants is reported. While the glassy alloy contains 24% chemically inactive metalloid elements, the powders are capable to completely decompose the $C_{32}H_{20}N_6Na_4O_{14}S_4$ azo dye in aqueous solution in short time, about 200 times faster than the conventional Fe powders. The metastable thermodynamic nature and the particle surface topography are the major factors controlling the chemical performance of the metallic glass. Our findings may open a new opportunity for functional applications of metallic glasses.

1. Introduction

Colorants and dyes are among the mostly utilized organic chemicals in modern industries for decorations and other purposes. But their applications often result in severe water pollution.^[1–5] Current approaches to degrade and detoxify the contaminants include reduction reaction by zero-valence metals,^[1–3] bacterial degradation^[4] and carbon sorbent absorption.^[5] Among the options, the zero valent metals have attracted a heightened industrial interest because of their low cost, efficient degradation capability and simple operations. Zero valent iron (ZVI), or crystalline elemental iron, in the form of powders, is the typical metal for water purification by decomposing the contaminants,^[1–3,6–8] but its fast corrosion leads to rapid decay of the efficiency.^[9] Noble metals have been combined with ZVI to improve the chemical stability and activity.^[7] The increased cost, however, limits their wide applications. Consequently, it is important to explore low cost, abundant materials that have

high efficiency in degrading the water contaminants.

The metallic glasses, unlike the crystalline metals in which the constituent atoms reside at thermodynamic equilibrium, are metastable materials in far-from-equilibrium states.^[10–12] The far-from-equilibrium nature is responsible for many excellent properties of metallic glasses that are unachievable in crystalline alloys.^[13,14] For example, the good chemical and catalytic properties of metallic glasses are well known.^[9,15–17] More interestingly, the compositions of the metallic glasses can

be widely tuned to improve their properties, especially when the glass forming ability is not the major concern. The intrinsic brittleness of some metallic glasses facilitates their subdivision into fine powders. The combination of metastable characteristics, widely tunable compositions, and intrinsic brittleness makes some of the metallic glasses very interesting catalytic materials for degrading the water contaminants.

In this paper, we report the excellent performance of a Fe-based metallic glass (hereafter, we denote it as G-ZVI) powders in degrading organic chemicals, by evaluating the decolorization capability in a Direct Blue Azo Dye $C_{32}H_{20}N_6Na_4O_{14}S_4$ aqueous solution. Different from the conventional wisdom, the G-ZVI powders were found to exhibit higher reaction activity than pure Fe, even though they contain 24 at.% metalloid elements such as Si and B. Our results are expected to open new opportunities for the functional applications of metallic glasses.

2. Results and Discussion

Two types of G-ZVI powders were prepared. One was fabricated using a high pressure argon gas atomization (GA) method. The other was prepared by ball-milling (BM) the glassy ribbon under Ar gas atmosphere. The morphologies of the GA and BM powders are shown in Figure 1a and b. It is evident that the particles are well dispersed and no aggregation can be observed in both types of powders. Compared with the GA powder particles whose surfaces are rounded and smooth (see the inset of Figure 1a), the BM particles appear to be rather irregular and many corrugations can be seen on their surfaces (see the inset of Figure 1b). The size distributions of the powders are presented in Figure 1c and d, respectively. For both powders, the distribution is narrow and the average diameter of the GA

Dr. J. Q. Wang, Dr. Y. H. Liu, Prof. M. W. Chen,
Prof. D. V. Louzguine-Luzgin, Prof. A. Inoue, Prof. J. H. Perepezko
WPI Advanced Institute of Materials Research
Tohoku University
Sendai 980-8577, Japan
E-mail: junqiangwang@wpi-aimr.tohoku.ac.jp; yhliu78@gmail.com
Prof. G. Q. Xie, Prof. A. Inoue
Institute for Materials Research
Tohoku University
Sendai 980-8577, Japan
Prof. J. H. Perepezko
Department of Materials Science and Engineering
University of Wisconsin-Madison
1509 University Avenue, Madison, WI 53706, USA



DOI: 10.1002/adfm.201103015

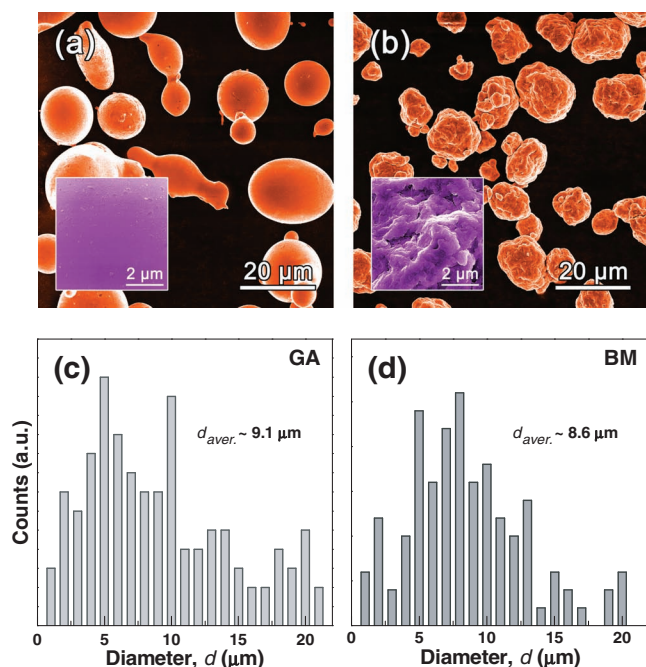


Figure 1. Particle morphologies of the gas-atomized (GA) (a) and ball-milled (BM) (b) glassy $\text{Fe}_{73}\text{Nb}_3\text{Si}_7\text{B}_{17}$ powders. The insets highlight the details of the surfaces. c,d) The respective distribution of particle sizes of the GA and BM powders.

powder is estimated to be about 9.1 μm, almost identical to that of the BM powder (~8.6 μm).

The appearance of the Azo Dye solution is shown in Figure 2a. Before the treatment by the G-ZVI powders, the characteristic absorption peak arising from the “–N=N–” azo bonding locates around 580 nm (see for example the black curve in Figure 2b) and makes the solution show dark blue color. The absorption intensity is proportional to the azo dye concentration and decreases along with the degradation progress.^[20] The UV spectra of the solutions treated by GA powders for different times at room temperature are shown in Figure 2b. The reaction between Fe and Azo Dye is a type of redox reaction, in which Fe atoms lose 2 or 3 electrons to form Fe^{2+} or Fe^{3+} ions and the –N=N– bond gets 4 electrons, becoming –NH₂.^[6,20] With the prolonged treatment time, the absorption peak becomes weaker and weaker, and an obvious peak shift cannot be observed, indicating the continuous degradation of the Azo Dye. As shown on the right in Figure 2a, the Azo Dye can be completely degraded by the G-ZVI. The solution becomes fully transparent without any color, and no characteristic peaks can be observed from its UV absorption spectrum (Figure 2b). This indicates that the G-ZVI has good reaction activity and can thoroughly decompose the Azo Dye. The UV absorption spectra for the solutions treated by the BM powder are presented in Figure 2c. As can be seen, the absorption peak fades out very quickly during the initial 20 min and disappears within 60 min. The solutions first become light red and then totally transparent. To quantitatively compare the efficiency of the G-ZVIs, the normalized intensities of the UV absorption peaks are plotted in Figure 2d as function of treatment time, together with that by the pure Fe powder. The

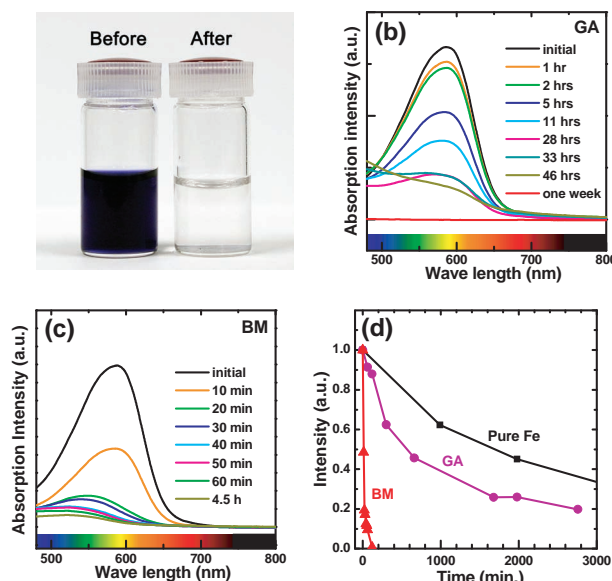


Figure 2. a) The appearance and color of the Azo Dye Direct Blue 6 solution before and after the treatment by the G-ZVI powder. b, c) The changes of UV absorption spectra along with the treatment by GA and BM powders, respectively. d) The normalized peak intensity at 580 nm as function of treatment time for three different powders. The treatments were performed at room temperature.

time when the peak intensity becomes half of the initial one is used as a measure of the degradation efficiency. For BM G-ZVI, the time is about 10 min, which is significantly shorter than that for GA G-ZVI (~600 min) and pure Fe powder (~2000 min). These results demonstrate that the G-ZVI synthesized by ball milling has high efficiency, about 60 times faster than the gas-atomized G-ZVI and 200 times faster than the Fe powders.

3. Discussion

To understand the difference of the reaction kinetics of the two G-ZVIs, we measured the absorption spectra of the solutions at various temperatures. Figure 3(a) and (b) show the intensity vs treatment time at different temperatures for GA and BM G-ZVI powders, respectively. The decay behavior can be well fitted by an exponential function, $I = I_0 + I_1 e^{-t/t_0}$,^[21] where I is the normalized intensity of the absorption peak, I_0 and I_1 are fitting constants, t is the degradation time, and t_0 is the time when the intensity decrease to e^{-1} of the initial state and can be derived by fitting the data points. Since the reaction is a thermally activated process, the thermal activation energy barrier ΔE can be evaluated with the Arrhenius-type equation, $t_0 = \tau_0 \exp(\Delta E/RT)$, where τ_0 is a time pre-factor, R the gas constant. Figure 3c,d presents the Arrhenius plots of $\ln t_0$ vs $1/T$ for the GA and BM glassy powders, respectively. The ΔE value for BM G-ZVI powders is 78 kJ mol⁻¹, while that of GA G-ZVI powder is 114 kJ mol⁻¹. The different activation energies indicate that the degradation reaction is much easier to happen on the BM particles.

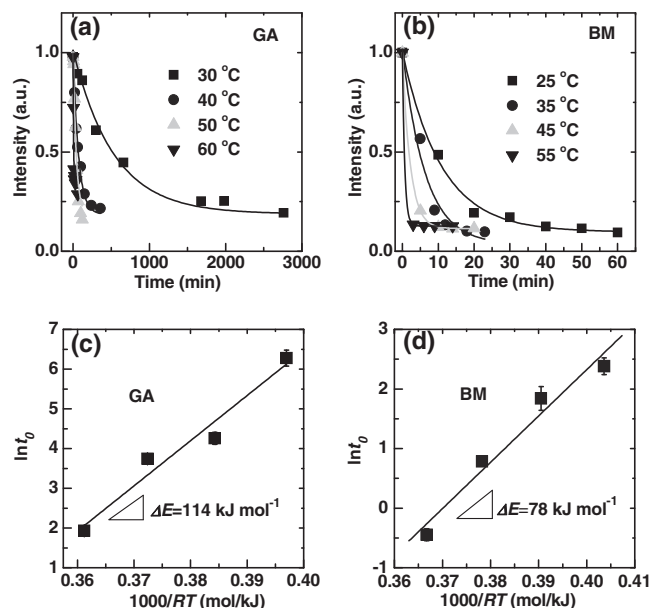


Figure 3. The normalized UV absorption intensity at 580 nm versus the reaction time at different temperatures for the GA (a) and BM (b) G-ZVI powders. The solid lines are exponential decay fitting to the data points. c, d) Plot of the decay time (t_0) versus temperature for GA and BM G-ZVI powders, respectively. The solid lines are the fitting by Arrhenius-type equation to yield the activation energy.

As shown in the insets of Figure 1a, the surfaces of GA particles are smooth. However, numerous nanoscale protrusions and corrugations can be seen on the surfaces of BM particles (inset of Figure 1b). Therefore, the surface area of the BM powder is dramatically enhanced by the nano-scale features and the reaction can occur on more sites than that on the GA powder. **Figure 4a** and **b** demonstrate the post-reaction particle topography for the two types of powders. In the case of GA powders, the reaction only happens on sparse sites of the GA particles (Figure 4a). However, for the BM particles, the reaction product distributes uniformly on all the surface of the particles (Figure 4b). This explicitly indicates that nanoscale surface features provide more active sites for the reaction to proceed and thus improve the degradation efficiency. Moreover, it is known that

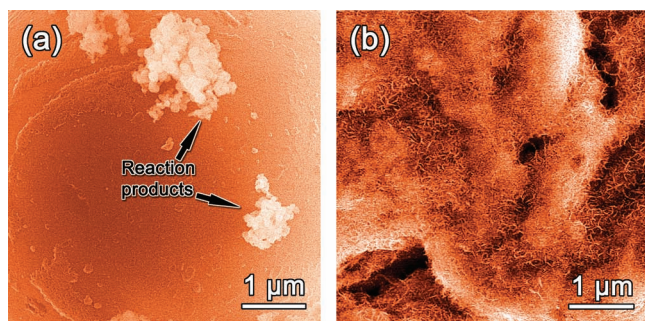


Figure 4. Surface morphologies of the a) GA and b) BM particles after reaction. Note that the reaction products distribute sparsely on the GA particle, while they distribute homogeneously on the surface of BM particles.

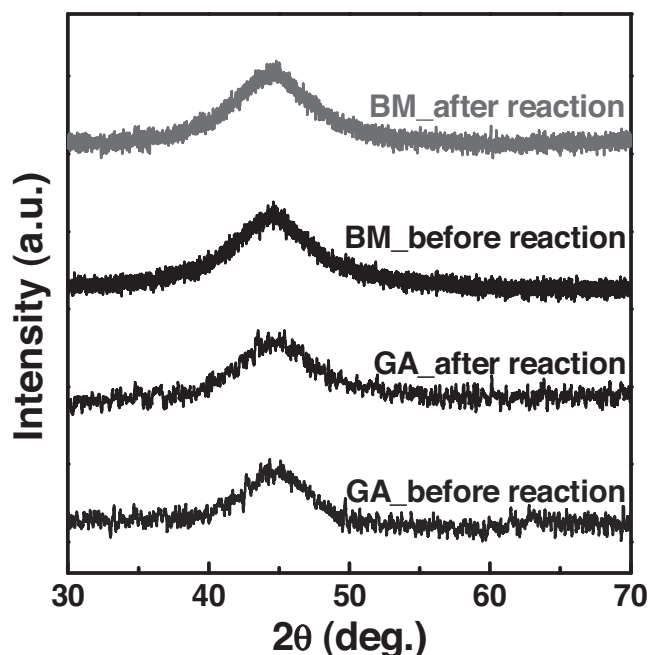


Figure 5. The XRD curves of the powders before and after reaction show that the powders maintain the glassy state.

the particles undergo intense plastic deformation during ball-milling, and huge residual stress can be built up within the particles. The strong residual stress and stored plastic deformation energy may also facilitate the reaction activity and contribute to the low ΔE for BM glassy powders.

Finally, it is interesting to note that even though the G-ZVI powders contain metalloid elements as much as 20 at.%, they are still able to degrade the dye efficiently. This indicates that the metastable bonding between the atoms in Fe-based metallic glasses permits the Fe atoms to keep high reaction activity in the dye solution. This is consistent with a recent report that the nanocrystallized Fe sample is much less active in the reaction compared to the glassy one.^[17] The significantly different activation energies and degradation speed for the two kinds of glassy powders suggest that, in addition to the metastable thermodynamic state of the glassy powders, the reaction kinetics is associated with the routes they are made and thereby the particle surface topography, since no obvious difference in atomic structures can be found between the two type of powders, as shown in **Figure 5**. Moreover, after reaction, the powders remain amorphous and no obvious changes can be found in the XRD curves as is shown in **Figure 5**. This indicates that the reaction solely consumes the surface constituent atoms of the G-ZVI particles, but does not alter the basic atomic structures.

4. Conclusion

Two types of G-ZVIs, the gas atomized and ball milled powders, were fabricated and their efficiency and reaction kinetics in degrading organic chemicals were systematically investigated by evaluating their decolorization capability in a $\text{C}_{32}\text{H}_{20}\text{N}_6\text{Na}_4\text{O}_{14}\text{S}_4$

aqueous solution. While they contains 24 at.% chemically inactive metalloid elements, the G-ZVIs exhibit excellent degradation efficiency, both of the powders can completely decompose the “-N = N-” bond. The higher efficiency of ball-milled powder is associated with its large surface area of many nanoscale corrugations. Our findings are expected to open a new opportunity for the functional applications of metallic glasses.

5. Experimental Section

The $\text{Fe}_{73}\text{Si}_{17}\text{Nb}_3$ ingot was prepared by arc melting high purity elements in a Ti-gettered argon atmosphere. Two types of G-ZVI powders were prepared. One was fabricated using a high pressure argon gas atomization (GA) method,^[18] in which the ingot was melted by induction heating and the alloy melt was injected through a nozzle with diameter of 0.8 mm by flowing argon gas with a dynamic pressure of ~8 MPa. The other was prepared by ball-milling (BM) the glassy ribbon under Ar gas atmosphere. The glassy state of the powders was characterized by X-ray diffraction (XRD) and differential scanning calorimetry (DSC).^[19] The particle surface topography were inspected by scanning electron microscopy (SEM). The aqueous solution of $\text{C}_{32}\text{H}_{20}\text{N}_6\text{Na}_4\text{O}_{14}\text{S}_4$ dye (Direct Blue 6) with concentration of 200 mg L^{-1} was used to evaluate the reaction activity. For each degradation experiment, 0.67 g glassy powder was added into 50 mL solution. Commercial Fe powders with particle size around 325 mesh were also tested for comparison. The reacted solution were taken out and filtered to measure the absorption spectra using an ultraviolet-visible absorption spectrophotometer (JASCO V-650 Spectrophotometer).

Acknowledgements

The authors appreciate the experimental help from Dr. N. Chen, Dr. J. L. Kang, and Dr. V. Zadorozhnyy. This work was supported by

World Premier International Research Center Initiative (WPI), MEXT, Japan.

Received: December 13, 2011
Published online: April 5, 2012

- [1] W. X. Zhang, *J. Nanoparticle Res.* **2003**, *5*, 323.
- [2] W. A. Arnold, A. L. Roberts, *Environ. Sci. Technol.* **1998**, *32*, 3017.
- [3] J. P. Fennelly, A. L. Roberts, *Environ. Sci. Technol.* **1998**, *32*, 1980.
- [4] S. D. Kalme, G. K. Parshetti, S. U. Jadhav, S. P. Govindwar, *Bioresource Tech.* **2007**, *98*, 1405.
- [5] N. K. Amin, *J. Hazardous Mater.* **2009**, *165*, 52.
- [6] A. Agrawal, P. G. Tratnyek, *Environ. Sci. Tech.* **1996**, *30*, 153.
- [7] C. B. Wang, W. X. Zhang, *Environ. Sci. Tech.* **1997**, *31*, 2154.
- [8] Z. Xiong, D. Zhao, G. Pan, *Water Res.* **2007**, *41*, 3497.
- [9] A. Baiker, *Faraday Discuss. Chem. Soc.* **1989**, *87*, 239.
- [10] A. Inoue, *Acta Mater.* **2000**, *48*, 279.
- [11] A. L. Greer, *Science* **1995**, *267*, 1947.
- [12] W. L. Johnson, *MRS Bull.* **1999**, *24*, 42.
- [13] A. Inoue, A. Takeuchi, *Acta Mater.* **2011**, *59*, 2243.
- [14] W. H. Wang, *Adv. Mater.* **2009**, *21*, 4524.
- [15] T. Katona, A. Molnar, *J. Catal.* **1995**, *153*, 333.
- [16] M. Carmo, R. C. Sekol, S. Ding, G. Kumar, J. Schroers, A. D. Taylor, *ACS Nano* **2011**, *5*, 2979.
- [17] C. Q. Zhang, H. F. Zhang, M. Q. Lv, Z. Q. Hu, *J. Non-Cryst. Solids* **2010**, *356*, 1703.
- [18] G. Q. Xie, D. V. Louzguine-Luzgin, H. Kimura, A. Inoue, *Appl. Phys. Lett.* **2007**, *90*, 241902.
- [19] G. Q. Xie, D. V. Louzguine-Luzgin, A. Inoue, *J. Alloys Comp.* **2011**, *509s*, S214.
- [20] J. Cao, L. Wei, Q. Huang, L. Wang, S. Han, *Chemosphere* **1999**, *38*, 565.
- [21] H. Y. Shu, M. C. Chang, H. H. Yu, W. H. Chen, *J. Colloid Interface Sci.* **2007**, *314*, 89.